# Stepwise Filtering of the Internal Layers of Dendrimers by Transverse Relaxation-Edited NMR

Luiz F. Pinto, Ricardo Riguera,* and Eduardo Fernandez-Megia*

Department of Organic Chemistry and Center for Research in Biological Chemistry and Molecular Materials (CIQUS), University of Santiago de Compostela, Jenaro de la Fuente s/n, 15782 Santiago de Compostela, Spain.

*Supporting Information Placeholder*

**ABSTRACT:** The characteristic distribution of transverse relaxation times ($T_2$) within dendrimers (lower values at the core than the periphery) can be exploited in $T_2$-edited 1D and 2D NMR experiments for the stepwise filtering of internal nuclei according to their topology within the dendritic structure. The resulting filtered spectra, which can be conceived as corresponding to virtual hollow dendrimers, benefit from reduced signal overlapping and so facilitate signal assignment and characterization. The generality of the method as a powerful tool in structural and end-group analysis has been confirmed with various dendritic families and nuclei ($^1$H, $^{13}$C, $^{31}$P).

Dendrimers are synthetic tree-like macromolecules composed of repetitive layers of branching units that are prepared in a controlled iterative fashion, through generations with precise molecular weight and discrete properties. As a function of generation, globular architectures and sizes emerge in the nanoscale that render dendrimers attractive for many applications in the fields of catalysis, nanomaterials and nanomedicine.[1] Nuclear magnetic resonance (NMR) is the technique of choice for routine structural characterization of dendrimers.[2] NMR relaxation is also recognized as a versatile way to study their dynamics by measuring longitudinal ($T_1$) and transverse ($T_2$) relaxation times, and nuclear Overhauser effect (NOE).[3] In spite of conflicting theoretical models (dense-core[4] *vs* dense-shell[5]) that initially obscured the dynamical analysis of dendrimers, a consensus has been later adopted around the dense-core model.[6] We have recently reported a NMR relaxation study on the dynamics of dendrimers ($^1$H and $^{13}$C $T_1$ and $T_2$, NOE) showing that slower internal dynamics are accompanied by a reduction of $T_2$ values on going from the periphery to the core.[7] Herein we report that advantage can be taken of this characteristic distribution of $T_2$ for the stepwise filtering of the internal dendritic layers in 1D and 2D NMR spectra as a powerful tool for easier signal assignment and characterization.

In NMR experiments, spin systems in a non-equilibrium condition after a 90° pulse immediately return to equilibrium by longitudinal and transverse relaxation. The intensity of the transverse component of the magnetization decays to zero by spin-spin relaxation according to equation (1) $I_{xy} = I_0 \cdot \exp(-t/T_2)$, where $I_0$ is the intensity at time $t = 0$.[8] In complex mixtures of species with different $T_2$ values (*e.g.*; macromolecules with low $T_2$ and low molecular weight molecules with large $T_2$), the resonances of lowest $T_2$ can be filtered from the NMR spectra by means of spin-echo pulse sequences, typically the Carr–Purcell–Meiboom–Gill [CPMG, $90^o_x\text{-}(\tau\text{-}180^o_y\text{-}\tau)_n$; where $2\tau$ is a fixed echo time, $n$ is the number of echoes, and $2\tau n$ the total echo duration].[9] CPMG and related sequences[10] keep the magnetization in the transverse plane for a time $t$ equal to $2\tau n$ before FID acquisition, allowing the magnetization of each nuclei to independently decay according to their characteristic $T_2$ values (the larger the $T_2$, the slower the decay). Eventually, after a certain time $t$ (known as $T_2$ or CPMG filter), differences in $T_2$ can be exploited for the selective suppression of the NMR signals of macromolecular species while enhancing the detection of small molecules. Successful examples of this filtering strategy include the metabolic profiling of cells, tissues, and biological fluids;[11] where $T_2$ filters at least 5-7 times the $T_2$ of the signals to filter are implemented to ensure their 99.3-99.9% suppression (eq. 1). Application of the same concept to the rich internal distribution of $T_2$ in dendrimers was envisaged as an opportunity for the stepwise filtering of the internal signals of lower $T_2$. The resulting filtered spectra, which can be conceived as corresponding to a collection of virtual hollow dendrimers, benefit from reduced signal overlapping, which facilitates NMR assignment and characterization.

The feasibility of the strategy was first demonstrated in $^1$H NMR with Fréchet-type poly(aryl ether) dendrimers.[12] Figure 1 depicts the structure and $^1$H NMR spectrum of a third generation (G3) poly(aryl ether) dendrimer, showing well-resolved benzylic (*a*, *bc*, *d*) and aromatic (*A*, *BD*, *C*, *Z*) protons. The potential of $T_2$ filters for the selective suppression of the $^1$H signals according to their topology within the dendritic structure (different $T_2$ values) was assessed by plotting the normalized $^1$H intensities ($I_{xy}/I_0$) as a function of the echo duration. As seen in Figure 1, the $I_{xy}/I_0$ for the different nuclei is reduced with the echo duration in a topology dependent fashion that ensured their stepwise selective suppression from the core to the periphery. Indeed, as indicated by color arrows in the $T_2$-filtered spectra, the sequential suppression of the aliphatic protons was possible by implementing increasing $T_2$ filters from 170 ms (core methyl) to 840 ms (benzylic *d*), 1.4 s (benzylic *bc*), and 3.4 s (benzylic *a*). Similarly, from the $I_{xy}/I_0$ plot of the aromatic signals, filters could be selected for their stepwise suppression from the core (*Z* protons) to the periphery, to finally afford a $^1$H NMR spectrum showing only the most exposed protons A (longest $^1$H $T_2$) after a 6.6 s filter (Figure 1).

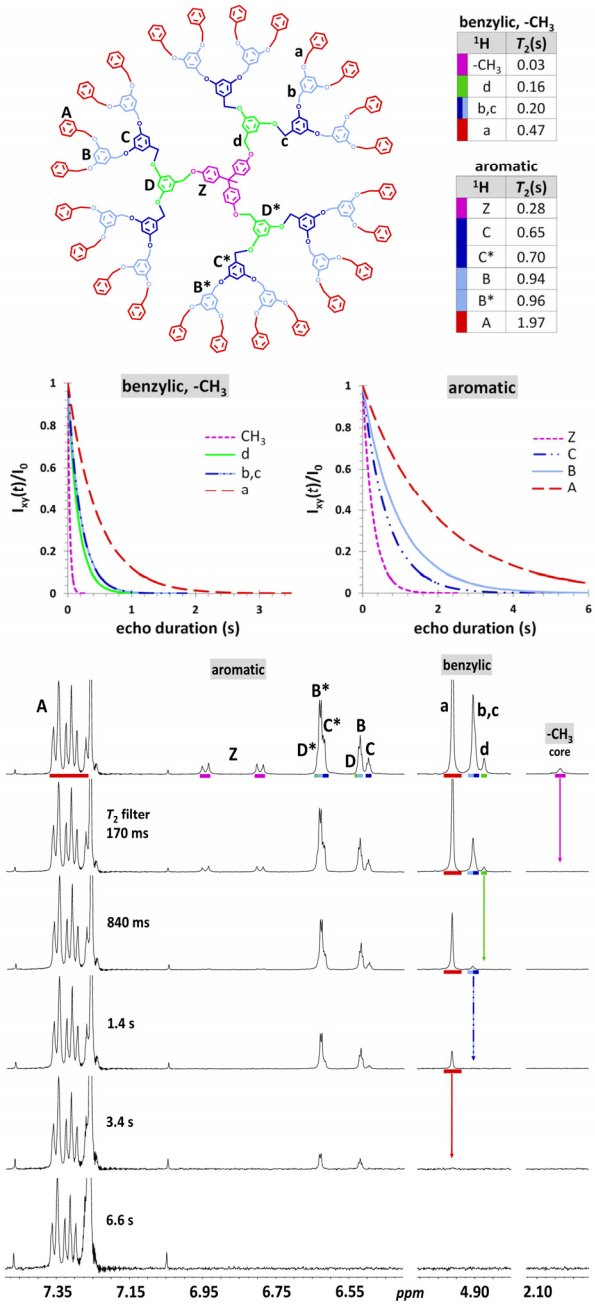


**Figure 1.** Top panel: Structure of G3 poly(aryl ether) dendrimer [1,1,1-tris(4'-hydroxyphenyl)ethane core], $^{1}H$ $T_2$ values and normalized $^{1}H$ intensities ($I_{xy}/I_0$) as a function of the echo duration. Bottom panel: $T_2$-filtered spectra (500 MHz, $CDCl_3$, 298 K).

Generality of the approach for filtering the NMR spectra of dendrimers was obtained by application to other classical dendritic families, including Majoral's phosphorus P-dendrimers[13] and Tomalia's poly(amido amine) (PAMAM).[14] In the first case, the similarity between all $^{1}H$ $T_2$ at the internal layers in a G2 dendrimer allowed their selective suppression with a $T_2$ filter of 3 s, which rendered a spectrum showing only the most peripheral aromatic and aldehyde signals (Figure 2). In a second step, filtering of the external aromatic protons was also possible with a longer 8 s filter (both filters account for *ca.* 6-times the longest $T_2$ signal to suppress). The fidelity of the strategy was demonstrated by application to $T_2$-filtered 2D NMR experiments where the CPMG sequence is used as an excitation block replacing the first excitation pulse.[15] For instance, the use of 3 and 8 s filters in a $T_2$-filtered COSY experiment selectively afforded the desired suppressions in G2 P-dendrimer (Figure S3).

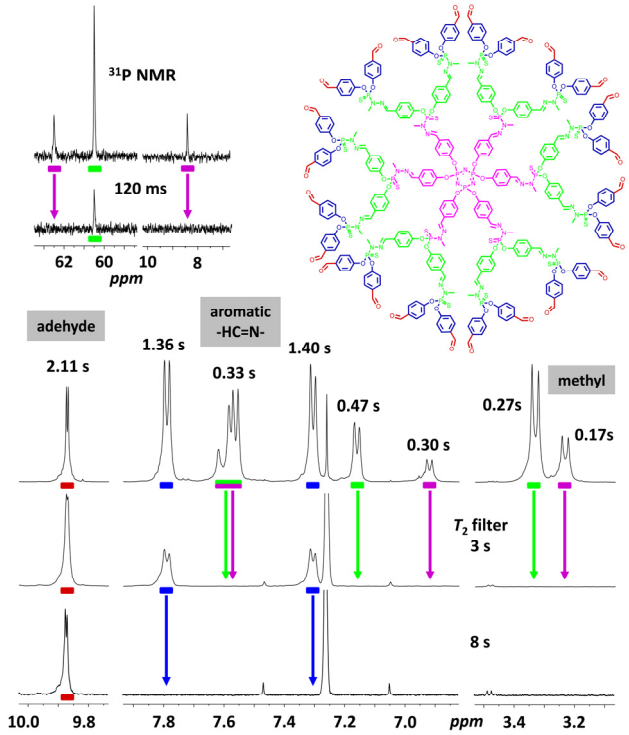


**Figure 2.** Structure of G2 P-dendrimer (cyclotriphosphazene core) carrying 24 peripheral aldehydes and $^{1}H$ and $^{31}P$ $T_2$-filtered spectra (500 MHz for $^{1}H$ and 202 MHz for $^{31}P$, $CDCl_3$, 298 K). $^{1}H$ $T_2$ values are shown above the $^{1}H$ spectra.

PAMAM illustrates a kind of dendrimers with low NMR resolution among nuclei at the different layers that complicates the straightforward identification of the external groups. This characteristic renders PAMAM especially suited to benefit from the selective suppression of broad internal signals by application of $T_2$ filters. In the absence of a detailed $^{1}H$ $T_2$ map available for PAMAM, we envisioned the direct implementation of a selection of $T_2$ filters as the most accelerated filtering strategy. Certainly, as seen in Figure 3 for G4 PAMAM, the application of four filters between 150 ms and 3 s allowed us to obtain a spectrum ($T_2$ filter 1 s) showing only the most peripheral protons, which remained partially hidden in the original spectrum.

The possibility of filtering internal layers in dendrimers without the necessity of previous knowledge of $T_2$ was also useful in the characterization and signal assignment of peripherally decorated dendrimers. With this aim, a G4 poly(propylene imine) (PPI) dendrimer[16] was decorated with 32 ibuprofen molecules (see the SI). Implementation again of four filters between 150 ms and 3 s resulted in the complete suppression of the internal PPI signals (300 ms filter) and the selective visualization of the resonances due to ibuprofen (Figure 4). Remarkably, fruitful characterization of the ibuprofen groups without interference of PPI signals was also possible by application of the very same 300 ms filter to a $T_2$-filtered COSY and a heteronuclear $^{1}H$-$^{13}C$ $T_2$-filtered HSQC (Figure 4). Since relaxation in $^{1}H$ heteronuclear 2D experiments (indirect detection) is governed by the $^{1}H$ nucleus, $T_2$ filters in HSQC experiments are determined according to $^{1}H$ $T_2$ values.

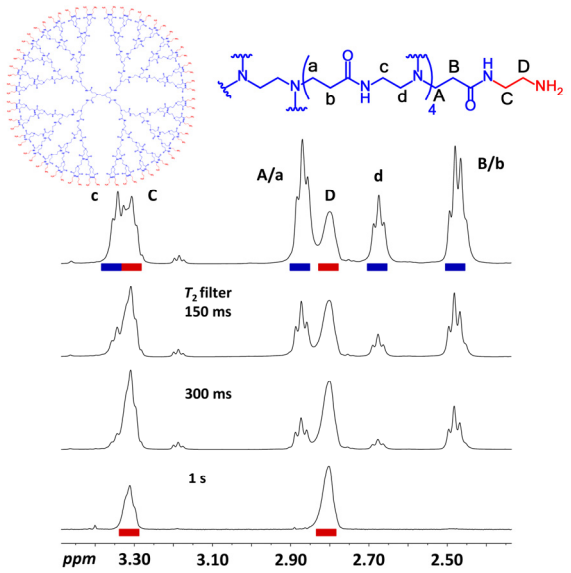


**Figure 3.** Structure of G4 PAMAM (ethylenediamine core) and $^1$H $T_2$-filtered NMR spectra (500 MHz, $CDCl_3$, 298 K).

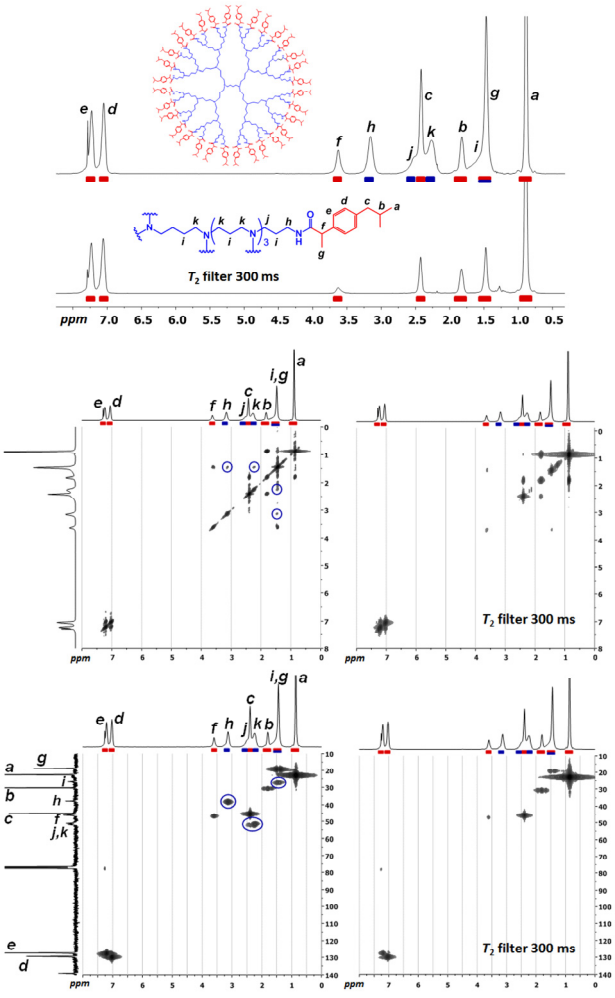


**Figure 4.** Top panel: structure of G4 PPI-ibuprofen (1,4-diaminobutane core) and $^1$H $T_2$-filtered NMR spectrum. Bottom panel: $T_2$-filtered COSY and $^1$H-$^{13}$C HSQC spectra showing in blue circles the PPI cross-peaks (500 MHz, $CDCl_3$, 298 K).

The potential of this filtering tool was further evaluated by application to a dendrimer for which $T_2$ data were available in the literature and hence, filters could be straight determined as 7×$T_2$ to ensure a 99.9% signal suppression (eq. 1). With this aim we selected a G4 PPI dendrimer decorated with triethylene glycol (TEG) groups previously reported by the groups of Ford and Zhu.[17] Figure 5 depicts the structure of PPI-TEG along with the $^1$H $T_2$ values in $D_2O$ (1 wt.%, 300 MHz) as described by the authors, namely protons *a* (1.21 s), *b* (0.29 s), *f* (0.16 s), *h* (30 ms), *i* (30 ms). According to these data, the stepwise suppression of *h*-*i*, *f*, and *b* was assessed with $T_2$ filters equal to 210 ms, 1.12 s, and 2.03 s. As expected, the two first filters proceeded very efficiently for the selective suppression of *h*-*i* and *f*. The third filter, however, failed in the goal to completely suppress proton *b*, suggesting a much longer $^1$H $T_2$ for this proton than the reported 0.29 s. Confirmation of this point was obtained by determining a $^1$H $T_2$ of 0.48 s. Indeed, application of a 3.4 s filter (equivalent to 7×0.48 s) afforded the pursued filtration and a spectrum showing only the outermost methyl protons *a*. The relatively small dependence of $T_2$ on the magnetic field[18] encouraged us to test the robustness of the method at different fields. To this end, the above $T_2$ filters determined at 300 MHz were implemented in a 500 MHz spectrometer. Gratifyingly, a clean stepwise suppression was revealed, demonstrating the utility of the tool with spectrometers operating at fields different to that used for the determination of $T_2$ (Figure S4).

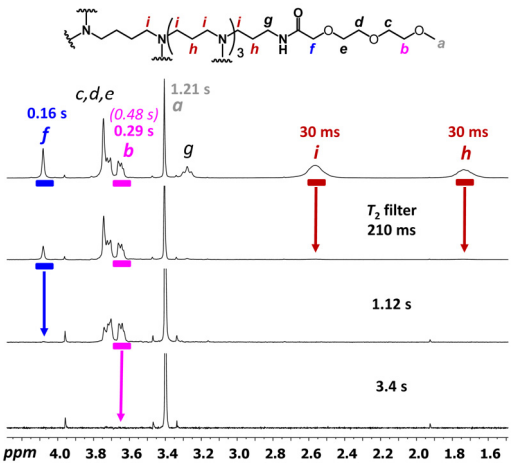


**Figure 5.** Structure of G4 PPI-TEG (1,4-diaminobutane core), $^1$H $T_2$ values, and $^1$H $T_2$-filtered NMR spectra (300 MHz, 1 wt.% in $D_2O$, 298 K).

A practical application of the $T_2$ filters involved the analysis of partially/incompletely functionalized dendrimers. For instance, it is known that the inherent toxicity of cationic aminodendrimers can be modulated by partial acetylation, which also results in increased solubility and reduced nonspecific targeting. Such a strategy has been thoroughly studied for PAMAM dendrimers with different degrees of acetylation.[19] A partially acetylated (70%) G4 PAMAM dendrimer was prepared following these procedures. Analysis of the $^1$H NMR spectrum of this sample showed extensive overlapping between peripheral non-acetylated end-groups and resonances from internal nuclei that complicated characterization (Figure 6). Suppression, however, of all resonances from internal layers was possible with a $T_2$ filter of 1.1 s, after which the presence of non-acetylated groups was unambiguously confirmed both by $^1$H NMR and a $T_2$-filtered COSY experiment (Figures 6 and S5). Application of the same concept is expected to aid analysis of end-group purity during the growing process of dendrimers and post-functionalization.

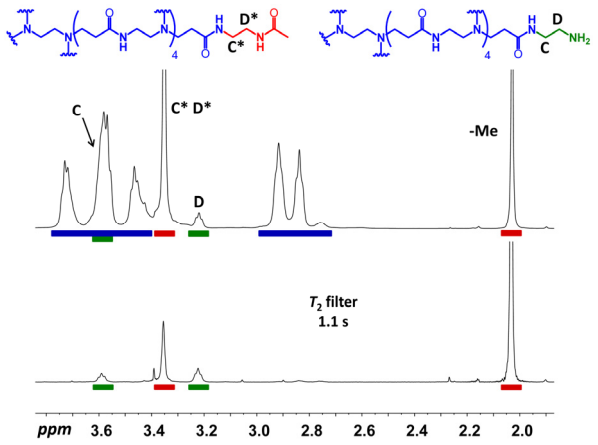


**Figure 6.** Structure of partially acetylated G4 PAMAM (ethylenediamine core) and $^{1}H$ $T_2$-filtered NMR spectrum (500 MHz, $D_2O$, pD 3.8, 298 K).

Lastly, considering the relevance of the NMR spectroscopy of nuclei different to $^{1}H$ in the characterization of dendrimers, we decided to test the viability of this $T_2$-filtering strategy in $^{13}C$ and $^{31}P$ NMR of dendrimers. $^{13}C$ is especially interesting because of its higher resolution compared to $^{1}H$, while $^{31}P$ was selected to illustrate the relevance of alternative nuclei in the analysis of heteroatom-containing dendrimers, such as the P-dendrimers. With this aim, a G2 poly(aryl ether) and a G2 P-dendrimer carrying 24 peripheral groups were submitted to $^{13}C$ and $^{31}P$ $T_2$-filtered NMR experiments, respectively. Figures 2 and S6 confirm the selective suppression of the resonances due to the internal layers in a stepwise fashion according to their characteristic $T_2$ values, greatly facilitating the signal assignment of both nuclei.

In conclusion, the characteristic distribution of $T_2$ values within dendrimers (lower values at the core than the periphery) can be exploited in $T_2$-edited NMR experiments for the stepwise filtering of nuclei at the internal layers. The resulting spectra corresponding to virtual hollow dendrimers benefit from reduced signal overlapping and facilitate signal assignment and characterization. The generality of the method has been confirmed with various dendritic families, nuclei ($^{1}H$, $^{13}C$, $^{31}P$), and 2D experiments (COSY and HSQC). In cases where no previous knowledge of $T_2$ is available, an accelerated strategy has been developed by implementing selected filters: four between 150 ms and 3 s in the case of $^{1}H$. Application of $T_2$ filters is envisaged to aid structural and end-group analysis in related dendritic structures, including block, dendronized, and hyperbranched polymers.

## ASSOCIATED CONTENT

### Supporting Information

Synthesis and characterization of dendrimers, NMR methods, and Figures. This material is available free of charge via the Internet at http://pubs.acs.org.

## AUTHOR INFORMATION

### Corresponding Author

ricardo.riguera@usc.es; ef.megia@usc.es

## ACKNOWLEDGMENT

This work was financially supported by the Spanish Government (CTQ2009-10963, CTQ2012-34790, CTQ2009-14146-C02-02, CTQ2012-33436) and the Xunta de Galicia (10CSA209021PR and CN2011/037). Luiz F. Pinto thanks the Portuguese Foundation for Science and Technology (FCT MCTES) for a Ph.D. grant (SFRH/BD/37341/2007). The authors thank Dr. Juan Correa (CIQUS) for helpful discussions and Dr. Manuel Martin-Pastor (NMR Unit RIAIDT) for help in implementing the $T_2$-filtered HSQC pulse sequence.

## REFERENCES

(1) (a) Sousa-Herves, A.; Riguera, R.; Fernandez-Megia, E. *New J. Chem.* **2012**, *36*, 205. (b) Röglin, L.; Lempens, E. H. M.; Meijer, E. W. *Angew. Chem., Int. Ed.* **2011**, *50*, 102. (c) Caminade, A.-M.; Turrin, C.-O.; Laurent, R.; Ouali, A.; Delavaux-Nicot, B. Dendrimers: Towards Catalytic, Material and Biomedical Uses; John Wiley & Sons, Ltd: Chichester, UK., 2011. (d) Astruc, D.; Boisselier, E.; Ornelas, C. *Chem. Rev.* **2010**, *110*, 1857. (e) Menjoge, A. R.; Kannan, R. M.; Tomalia, D. A. *Drug Discovery Today* **2010**, *15*, 171. (f) Vögtle, F.; Richardt, G.; Werner, N. Dendrimer Chemistry; Wiley-VCH: Weinheim, 2009. (g) Rosen, B. M.; Wilson, C. J.; Wilson, D. A.; Peterca, M.; Imam, M. R.; Percec, V. *Chem. Rev.* **2009**, *109*, 6275. (h) Lee, C. C.; MacKay, J. A.; Fréchet, J. M. J.; Szoka, F. C. *Nat. Biotechnol.* **2005**, *23*, 1517.

(2) Caminade, A.-M.; Laurent, R.; Majoral, J.-P. *Adv. Drug Delivery Rev.* **2005**, *57*, 2130.

(3) (a) Novoa-Carballal, R.; Säwén, E.; Fernandez-Megia, E.; Correa, J.; Riguera, R.; Widmalm, G. *Phys. Chem. Chem. Phys.* **2010**, *12*, 6587. (b) Moreno, K. X.; Simanek, E. E. *Macromolecules* **2008**, *41*, 4108. (c) Fernandez-Megia, E.; Correa, J.; Riguera, R. *Biomacromolecules* **2006**, *7*, 3104. (d) Chai, M.; Niu, Y.; Youngs, W. J.; Rinaldi, P. L. *J. Am. Chem. Soc.* **2001**, *123*, 4670. (e) Meltzer, A. D.; Tirrell, D. A.; Jones, A. A.; Inglefield, P. T.; Hedstrand, D. M.; Tomalia, D. A. *Macromolecules* **1992**, *25*, 4541.

(4) Lescanec, R. L.; Muthukumar, M. *Macromolecules* **1990**, *23*, 2280.

(5) de Gennes, P. G.; Hervet, H. *J. Phys., Lett.* **1983**, *44*, 351.

(6) Ballauff, M.; Likos, C. N. *Angew. Chem., Int. Ed.* **2004**, *43*, 2998.

(7) Pinto, L. F.; Correa, J.; Martin-Pastor, M.; Riguera, R.; Fernandez-Megia, E. *J. Am. Chem. Soc.* **2013**, *135*, 1972.

(8) Rabenstein, D. L. *J. Chem. Ed.* **1984**, *61*, 909.

(9) (a) Meiboom, S.; Gill, D. *Rev. Sci. Instrum.* **1958**, *29*, 688. (b) Carr, H. Y.; Purcell, E. M. *Phys. Rev.* **1954**, *94*, 630.

(10) (a) Aguilar, J. A.; Nilsson, M.; Bodenhausen, G.; Morris, G. A. *Chem. Commun.* **2012**, *48*, 811. (b) Rastrelli, F.; Jha, S.; Mancin, F. *J. Am. Chem. Soc.* **2009**, *131*, 14222.

(11) Novoa-Carballal, R.; Fernandez-Megia, E.; Jimenez, C.; Riguera, R. *Nat. Prod. Rep.* **2011**, *28*, 78.

(12) Hawker, C. J.; Fréchet, J. M. J. *J. Am. Chem. Soc.* **1990**, *112*, 7638.

(13) (a) Launay, N.; Caminade, A.-M.; Majoral, J. P. *J. Organomet. Chem.* **1997**, *529*, 51. (b) Launay, N.; Caminade, A.-M.; Lahana, R.; Majoral, J.-P. *Angew. Chem., Int. Ed.* **1994**, *33*, 1589.

(14) (a) Tomalia, D. A.; Naylor, A. M.; III, W. A. G. *Angew. Chem., Int. Ed.* **1990**, *29*, 138. (b) Tomalia, D. A.; Baker, H.; Dewald, J.; Hall, M.; Kallos, G.; Martin, S.; Roeck, J.; Ryder, J.; Smith, P. *Polym. J.* **1985**, *17*, 117.

(15) Williams, P. G.; Saunders, J. K.; Dyne, M.; Mountford, C. E.; Holmes, K. T. *Magn. Reson. Med.* **1988**, *7*, 463.

(16) (a) de Brabander-van den Berg, E. M. M.; Meijer, E. W. *Angew. Chem., Int. Ed.* **1993**, *32*, 1308. (b) Buhleier, E.; Wehner, W.; Vögtle, F. *Synthesis* **1978**, 155.

(17) (a) Baille, W. E.; Malveau, C.; Zhu, X. X.; Kim, Y. H.; Ford, W. T. *Macromolecules* **2003**, *36*, 839. (b) Kreider, J. L.; Ford, W. T. *J. Polym. Sci., Part A: Polym. Chem.* **2001**, *39*, 821.

(18) Kowalewski, J.; Mäler, L. *Nuclear Spin Relaxation in Liquids: Theory, Experiments, and Applications*; CRC Press: Boca Raton, 2006.

(19) (a) Kolhatkar, R. B.; Kitchens, K. M.; Swaan, P. W.; Ghandehari, H. *Bioconjugate Chem.* **2007**, *18*, 2054. (b) Majoros, I. J.; Keszler, B.; Woehler, S.; Bull, T.; Baker Jr., J. R. *Macromolecules* **2003**, *36*, 5526.

Table of Contents artwork